Effects on Molecular Association, Chelate Conformation, and Reactivity toward Substitution in Cu(5-X-salen) Complexes, salen^{2-} = *N,N'*-Ethylenebis(salicylidenaminato), X = H, CH_3O, and Cl: Synthesis, X-ray Structures, and EPR Investigations

Mohan M. Bhadbhade and D. Srinivas*

Discipline of Coordination Chemistry, Central Salt & Marine Chemicals Research Institute, Gijubhai Bhadheka Marg, Bhavnagar-364 002, India

Received April 6, 1993®

Three copper(II) complexes, Cu(5-X-salen), where salen^{2-} = *N,N'*-ethylenebis(salicylidenaminato) and X = H (**1**), CH_3O (**2**), or Cl (**3**), have been synthesized and characterized by various physicochemical techniques. Single crystal X-ray data of the complexes are as follows: **1**, $C_{16}H_{14}N_2O_2Cu$, monoclinic $C2/c$, a = 26.658(7) Å, b = 6.983(1) Å, c = 14.719(2) Å, β = 97.42(2)°, V = 2717(6) Å^3, Z = 8, R = 0.038 (R_w = 0.058); **2**, $C_{18}H_{18}N_2O_4Cu{\cdot}CH_3OH$, monoclinic $P2_1/n$, a = 11.061(3) Å, b = 7.537(6) Å, c = 21.765(5) Å, β = 92.86(2)°, V = 1812(2) Å^3, Z = 4, R = 0.066(R_w = 0.067); **3**, $C_{16}H_{12}N_2O_2Cl_2Cu$, triclinic $P\bar{1}$, a = 8.318(1) Å, b = 9.502(4) Å, c = 11.016(4) Å, α = 63.78(4)°, β = 75.62(3)°, γ = 78.83(4)°, V = 753(15) Å^3, Z = 2, R = 0.039 (R_w = 0.059). In solid state, **1** exists as strong dimers (Cu···O1′ = 2.414(2) Å) whereas **2** forms weak dimers (Cu···O1′ = 2.801(7) Å) intermolecularly bridged through phenolate oxygen and **3** is essentially a monomer. Copper is tetragonally distorted square pyramidal in **1** and **2** and tetrahedrally distorted square planar in **3**. Complexes exhibit color isomerism and solvatochromism in both solid and solution. EPR spectra are characterized by axial **g** and A_{Cu} tensors with $g_\parallel > g_\perp$ indicating that the unpaired electron occupies a "formal" d_{xy} orbital. A good correlation is obtained between the σ-basicity of the solvent and the spin Hamiltonian parameters. The mechanism for solvatochromism is discussed in terms of conformational changes and solvent coordination. EPR studies and extended Hückel molecular orbital calculations suggest that **3** forms more stable pyridine complexes than **1** and **2**. The effect of substitution on molecular electronic structure and reactivity toward solvent coordination is discussed.

Introduction

Environment around the metal center and conformational flexibility are the key factors for a metalloprotein to carry out a specific physiological function, e.g. dioxygen binding by hemoglobin and myoglobin, oxygen utilization by cytochrome P450 and cytochrome *c* oxidase, etc. Several model metal complexes containing porphyrin and Schiff base ligands have been synthesized and studied for their dioxygen uptake[1] and oxidative catalysis.[2-4] Flexibility of the ethylenediamine backbone in salen, as observed in a number of transition-metal complexes with bidentate oxygen ligands,[5] is responsible for its complexes to mimic the biological activity of proteins. Fine tuning of the electronic structure by introducing electron donating and withdrawing substituents in ligands is known to enhance the reactivity of the complexes.[6] However, reports dealing with the effect of substitution on molecular structure, spin state, electronic ground state, and reactivity of the complexes are very few.[6-10] With a view to understand the correlations between the molecular electronic structure and reactivity of the complexes better, we report here systematic spectroscopic and single-crystal X-ray structural investigations on three substituted salen complexes of Cu(II), Cu(5-X-salen), where X = H, CH_3O, and Cl, **1-3**.

The Schiff base ligand 5-X-salen coordinates through N_2O_2 donor atoms. The crystal structure of **1** is redetermined, as the earlier structure determinations[11,12] were based on two-dimensional X-ray data; **2** and **3** have not been reported so far. Complexes **1-3** exhibit color isomerism/solvatochromism in solid/solution state. Although NMR,[13] Mössbauer,[14] and electronic spectral[15] studies have been used to understand "solvatochromism", we report here for the first time EPR investigations on this phenomenon. Correlation between the spin Hamiltonian

* Abstract published in *Advance ACS Abstracts*, October 1, 1993.

(1) McLendon, G.; Martell, A. E. *Coord. Chem. Rev.* **1976**, *19*, 1. Niederhoffer, E. C.; Tommons, J. H.; Martell, A. E. *Chem. Rev.* **1984**, *84*, 137. Jones, R. D.; Summerville, D. A.; Basolo, F. *Chem. Rev.* **1979**, *79*, 139. Smith, T. D. *Coord. Chem. Rev.* **1981**, *39*, 295. Tovrog, B. S.; Kitko, D. J.; Drago, R. S. *J. Am. Chem. Soc.* **1976**, *98*, 5144.
(2) Groves, J. T.; Nemo, T. E.; Myers, R. S. *J. Am. Chem. Soc.* **1979**, *101*, 1032. Groves, J. T.; Kruper, W. J., Jr.; Haushalter, R. C. *J. Am. Chem. Soc.* **1980**, *102*, 6375. Groves, J. T.; Haushalter, R. C.; Nakamura, M.; Nemo, T. E.; Evans, B. J. *J. Am. Chem. Soc.* **1981**, *103*, 2884. Felton, R. H.; Owens, G. S.; Dolphin, D.; Fajer, J. *J. Am. Chem. Soc.* **1971**, *93*, 6332.
(3) Holm, R. H. *Chem. Rev.* **1987**, *87*, 1401.
(4) Srinivasan, K.; Michaud, P.; Kochi, J. K. *J. Am. Chem. Soc.* **1986**, *108*, 2309. Samsel, E. G.; Srinivasan, K.; Kochi, J. K. *J. Am. Chem. Soc.* **1985**, *107*, 7606. Dixit, P. S.; Srinivasan, K. *Inorg. Chem.* **1988**, *27*, 4507.
(5) Lauffer, R. B.; Heistand, R. H., II; Que, L., Jr. *Inorg. Chem.* **1983**, *22*, 50. Lloret, F.; Julve, M.; Mollar, M.; Castro, I.; Latorre, J.; Faus, J.; Solans, X.; Morgenstern-Badaran, I. *J. Chem. Soc., Dalton Trans.* **1989**, 729. Calligaris, M.; Manzini, G.; Nardin, G.; Randaccio, L. *J. Chem. Soc., Dalton Trans.* **1972**, 5430. Cummins, D.; McKenzie, E. D.; Milburn, H. *J. Chem. Soc., Dalton Trans.* **1976**, 130. Bailey, N. A.; Higson, B. M.; McKenzie, E. D. *J. Chem. Soc., Dalton Trans.* **1972**, 503. Kessel, S. L.; Emberson, R. M.; Debrunner, P. G.; Hendrickson, D. N. *Inorg. Chem.* **1980**, *19*, 1170.
(6) Corden, B. B.; Drago, R. S.; Perito, R. P. *J. Am. Chem. Soc.* **1985**, *107*, 2903.
(7) Williams, R. J. P. *Fed. Proc.* **1961**, *20*, 5.
(8) Hoard, J. L.; Hamor, M. J.; Hamor, T. A.; Caughey, W. S. *J. Am. Chem. Soc.* **1965**, *87*, 2312. Hoard, J. L. *Science (Washington, D.C.)* **1971**, *174*, 1295.
(9) Scheidt, W. R.; Reed, C. A. *Chem. Rev.* **1981**, *81*, 543.
(10) Kennedy, B. J.; McGrath, A. C.; Murray, K. S.; Skelton, B. W.; White, A. H. *Inorg. Chem.* **1987**, *26*, 483. Kennedy, B. J.; Brain, G.; Horn, E.; Murray, K. S.; Snow, M. R. *Inorg. Chem.* **1985**, *24*, 1647. Kennedy, B. J.; Fallon, G. D.; Gatehouse, B. M. K. C.; Murray, K. S. *Inorg. Chem.* **1984**, *23*, 580.
(11) Hall, D.; Waters, T. N. *J. Chem. Soc. A* **1960**, 2644.
(12) Pachler, V. K.; Stackelberg, M. V. *Z. Anorg. Allg. Chem.* **1960**, *305*, 286.
(13) Erlich, R. H.; Roach, E.; Popov, A. I. *J. Am. Chem. Soc.* **1970**, *92*, 4989. Erlich, R. H.; Popov, A. I. *J. Am. Chem. Soc.* **1971**, *93*, 5620. Greenbug, M. S.; Bodner, R. L.; Popov, A. I. *J. Phys. Chem.* **1973**, *77*, 2449. Krygowski, T. M.; Fawcett, W. R. *J. Am. Chem. Soc.* **1975**, *97*, 2143.
(14) Vértes, A.; Czakó-Nagy, I.; Burger, K. *J. Phys. Chem.* **1976**, *80*, 1314. de Vriés, J. L. K. F.; Trooster, J. M.; de Boer, E. *Inorg. Chem.* **1971**, *10*, 81. Burger, K.; Horvath, I. *Inorg. Chim. Acta* **1992**, *196*, 49.
(15) Waters, T. N.; Hall, D. *J. Chem. Soc. A* **1959**, 1200 and 1203.

0020-1669/93/1332-5458$04.00/0

equiv) results in the slow formation of **9** as shown by ^{1}H NMR spectroscopy. After 1 week about 60% of **3** had been converted to **9**. No side products could be detected.

In contrast to **3**, both **4** and **5** react readily with PPh_3 to give a complex identified as hydroxyruthenocene. This complex was also prepared recently by the action of Zn or NaHg on **5**.[14] The ^{1}H NMR spectra exhibits apparent triplets at 4.53 (2H) and 4.12 ppm (2H), respectively, and a singlet at 4.47 ppm (5H). There was no evidence, however, that PPh_3 was introduced into the C_5H_5 and/or C_5H_4O rings. A $^{31}P\{^1H\}$ NMR spectrum of the reaction mixture of **5** and PPh_3 was recorded and exhibited several singlets shifted down field to 66.9, 47.2, 42.7, and 31.7 ppm, respectively, with respect to PPh_3.

Crystal Structure of $[Ru(\eta^5\text{-}C_5H_4PCy_3)(\eta^5\text{-}C_5H_4OH)]PF_6$ (7). The structure of the cation is shown in Figure 1. The five-membered rings are nearly parallel to one another, the angle between the two planes being 3.5(2)°. The rings adopt an eclipsed conformation. Both OH and PCy_3 groups deviate from the cyclopentadienyl planes, in that O(1) and P(1) are bent away from the metal and are located 0.230(6) and 0.182(1) Å out of the ring planes, corresponding to a respective tilt of 7.4(2) and 8.1(4)°, respectively. The Ru–C distances are all similar, averaging to 2.189(4) Å, and can be compared to the Ru–C distances of $Ru(\eta^5\text{-}C_5H_5)_2$ (2.21 Å)[15] and $[Ru(\eta^5\text{-}C_5H_5)_2I]^+$ (2.20(2) Å).[16] There is a clear trend in the delocalized C–C bond distances within $C_5H_4PCy_3$ varying from 1.428(5) and 1.443(5) Å (C(1)–C(2) and C(5)–C(1), respectively) to 1.403(6) Å (C(3)–C(4)). The C–C distances in the C_5H_4OH ligand (average 1.421(5) Å) do not show this effect. In parent ruthenocene the average C–C distance is 1.43 Å.[15] The C(6)–O(1) distance is 1.292(6) Å and the P(1)–C(1) distance is 1.790(3) Å. The C_5H_4OH ring exhibits a disorder of the OH group with a site occupancy of 75% for O(1) being attached to C(6) and a site occupancy of 25% for O(2) being attached to the neighboring ring carbon C(10). In both orientations the hydroxy groups appear to be hydrogen bonded (O–H···F) to the PF_6^- anion. The cyclohexyl rings adopt the usual chair conformation. Selected bond distances may be found in Table V.

Crystal Structure of $[Ru(\eta^5\text{-}C_5H_5)(\eta^4\text{-}C_5H_4O)(P(OPh)_3)]PF_6$ (13). An ORTEP view of **13** is presented in Figure 2. The C_5H_5 and C_5H_4O rings are approximately staggered with respect to one another. The C_5H_4O ligand is distinctly bent and can be subdivided into two planes, one defined by C(7), C(8), C(9), and C(10) (butadiene fragment) and the other defined by C(7), C(6), O(1), and C(10). The angle between these planes is 23.7(2)° and somewhat larger than commonly encountered in complexes containing C_5H_4O as a ligand. In $Fe(\eta^4\text{-}C_5H_4O)(CO)_3$, $[Mo(\eta^5\text{-}C_5H_5)(\eta^4\text{-}C_5H_4O)(CO)_2]^+$, $[Ru(\eta^5\text{-}C_5H_5)(\eta^4\text{-}C_5H_4O)(CH_3CN)]^+$ (**2**), and $Ru(\eta^5\text{-}C_5H_5)(\eta^4\text{-}C_5H_4O)Br$ (**5**) this angle is 19.9, 18.0, 18.0, and 20.6°, respectively.[3-5,7] The diene C–C bonds adopt a short–long–short pattern (1.392(4) vs 1.450(4) Å) as was the case for the complexes mentioned above. The angle between the C_5H_5 plane and the butadiene fragment of C_5H_4O is 36.5(2)° (for comparison in **2** and **5** it is 36.0 and 36.2°, respectively).[4,6] The average Ru–C(C_5H_5) distance is 2.214(3) Å. The bond distances between Ru and the butadiene fragment are short for C(8) and C(9) being 2.167(3) and 2.181(3) Å, respectively, and long for C(7) and C(10) being 2.255(3) and 2.283(3) Å, respectively. The lengths of the C(6)–O(1) and Ru–P(1) bonds are 1.212(4) and 2.335(1) Å, respectively. The C–O distance is comparable to the corresponding distances in $Fe(\eta^4\text{-}C_5H_4O)(CO)_3$, $[Mo(\eta^5\text{-}C_5H_5)(\eta^4\text{-}C_5H_4O)(CO)_2]^+$, **2**, and **5** being 1.224(9), 1.212(4), 1.221(7), and 1.22(1) Å, respectively.[3-5,7] Selected bond distances may be found in Table V.

(14) Kirchner, K.; Kwan, K. S.; Taube, H. *Inorg. Chem.*, in press.
(15) Hardgrove, G. L.; Templeton, D. H. *Acta Crystallogr.* **1959**, *12*, 28.
(16) Sohn, Y. S.; Schlueter, A. W.; Hendrickson, D. N.; Gray, H. B. *Inorg. Chem.* **1974**, *13*, 301.

Table V. Selected Bond Lengths (Å)

	7	13	18
Ru–C(1)	2.182(3)	2.203(3)	2.214(13)
Ru–C(2)	2.165(3)	2.215(3)	2.195(11)
Ru–C(3)	2.187(4)	2.215(3)	2.173(10)
Ru–C(4)	2.204(4)	2.227(4)	2.163(13)
Ru–C(5)	2.195(3)	2.209(4)	2.195(12)
Ru–C(6)	2.224(4)		
Ru–C(7)	2.191(4)	2.255(3)	2.245(8)
Ru–C(8)	2.174(4)	2.167(3)	2.135(9)
Ru–C(9)	2.183(4)	2.181(3)	2.189(10)
Ru–C(10)	2.186(4)	2.283(3)	2.263(10)
Ru–P(1)		2.335(1)	
Ru–N(1)			2.064(7)
C(1)–C(2)	1.428(5)	1.400(5)	1.360(20)
C(2)–C(3)	1.416(5)	1.420(5)	1.390(20)
C(3)–C(4)	1.403(6)	1.415(5)	1.397(21)
C(4)–C(5)	1.416(5)	1.393(5)	1.401(19)
C(5)–C(1)	1.443(5)	1.436(5)	1.375(20)
C(6)–C(7)	1.391(6)	1.465(4)	1.516(13)
C(7)–C(8)	1.431(6)	1.397(4)	1.412(12)
C(8)–C(9)	1.421(7)	1.435(4)	1.428(14)
C(9)–C(10)	1.413(6)	1.387(4)	1.340(15)
C(10)–C(6)	1.400(6)	1.496(5)	1.500(14)
C(6)–O(1)	1.292(6)	1.212(4)	1.208(12)
P(1)–C(1)	1.790(3)		
P(1)–C(7)			1.782(8)
P(1)–C(11)	1.818(3)		1.789(9)
P(1)–C(17)	1.813(3)		1.796(10)
P(1)–C(23)	1.849(3)		1.799(9)
P(1)–O(2)		1.593(2)	
P(1)–O(3)		1.591(2)	
P(1)–O(4)		1.586(2)	
N(1)–C(29)			1.113(13)
C(29)–C(30)			1.466(15)

Crystal Structure of $[Ru(\eta^5\text{-}C_5H_5)(\eta^4\text{-}C_5H_3O\text{-}2\text{-}PPh_3)(CH_3CN)](PF_6)_2$ (18). A structural view of **18** is displayed in Figure 3. Similar to the structure of **13**, in **18** the two C_5 rings adopt an approximately staggered conformation. The PPh_3 substituent is bound in α position to the ketonic group 7.6(5)° out of plane of the butadiene unit bent away from the metal, the P(1)–C(7) distance being 1.782(8) Å. Though the bond distances of **18** are less accurate than in **13**, the dienone character of C_5H_4O is still apparent as indicated by the short–long–short pattern of the C–C distances. The C–C distances of the C_5H_4O ring are almost identical to the respective distances in the parent complex (**2**). The angle between the plane defined by the atoms C(7), C(8), C(9), and C(10) and the carbonyl functionality C(6)–O(1) is 16.3(5)° (for comparison in **2** this angle is 18.0°),[7] and the ketonic group is bent away from the metal. The C(6)–O(1) distance is 1.208(12) Å (1.221(7) Å in **2**). The angle between the C_5H_5 plane and the butadiene fragment of $C_5H_3O\text{-}2\text{-}PPh_3$ is 35.5(7)°. Acetonitrile is coordinated in η^1-fashion and practically linear (angle between N(1)-C(29)-C(30) is 179(1)°). The Ru–N(1) distance is 2.064(7) Å (in **2** this distance is 2.057(5) Å).[7] Other selected bond angles are shown in Table V.

Discussion

Our work on **1** and **2** has shown that in these complexes the C_5H_5 moiety is unusually reactive toward certain nucleophiles. Thus the reactions of **1** with PR_3 (R = Me, Cy, Ph) and $AsMe_3$ yielding 1,1′-disubstituted ruthenocenes of the type $[Ru(\eta^5\text{-}C_5H_4PR_3)(\eta^5\text{-}C_5H_4OH)]PF_6$ and $[Ru(\eta^5\text{-}C_5H_4AsMe_3)(\eta^5\text{-}C_5H_4OH)]PF_6$, respectively (reaction 3), proceed readily at room temperature. Similarly, the reaction of **2** with the more basic phosphines PMe_3 and PCy_3 results in the formation of the analogous products. However, when PPh_3 reacts with **2** a different pattern is followed, attack occurring exclusively on the ketone to form $[Ru(\eta^5\text{-}C_5H_5)(\eta^5\text{-}C_5H_3OH\text{-}2\text{-}PPh_3)]PF_6$ (**9**) (reaction 4). Further, when **2** is treated with $AsMe_3$, the corresponding product resulting

Table I. Summary of Crystallographic Data

	1	2	3
	Experimental Values		
molecular formula	$C_{16}H_{14}N_2O_2Cu$	$(C_{18}H_{18}N_2O_4Cu)\cdot(CH_4O)$	$C_{16}H_{12}N_2O_2Cl_2Cu$
molecular weight	329.8	421.9	398.7
space group	monoclinic, $C2/c$	monoclinic, $P2_1/n$	triclinic, $P\bar{1}$
cell parameters			
a (Å)	26.658(7)	11.061(3)	8.318(1)
b (Å)	6.983(1)	7.537(6)	9.502(4)
c (Å)	14.719(2)	21.765(5)	11.016(4)
α (deg)	90	90	63.78(4)
β (deg)	97.42(2)	92.86(2)	75.62(3)
γ (deg)	90	90	78.83(4)
V (Å^3)	2717(6)	1812(2)	753(15)
Z	8	4	2
no. of reflections and θ range (deg) used for unit cell parameters	25, 15–25	23, 8–12	21, 15–30
radiation used, λ (Å)	Cu Kα, 1.5418	Mo Kα, 0.7107	Cu Kα, 1.5418
D_{calc} (g cm^{-3})	1.613	1.540	1.758
absorption coeff, μ (cm^{-1})	22.71	12.34	54.62
temperature (K)	295	295	295
crystal color & descrptn	dark green plates	wine red needles	brown needles
crystal dimensions (mm)	0.18 × 0.18 × 0.05	0.30 × 0.08 × 0.04	0.40 × 0.10 × 0.06
	Data Collection		
diffractometer used	Enraf-Nonius CAD-4	Enraf-Nonius CAD-4	Enraf-Nonius CAD-4
scan mode	ω–2θ	ω–2θ	ω–2θ
absorption correction[18]	empirical	empirical	empirical
transmission min, max	74.0, 99.8	89.7, 93.6	87.4, 99.8
measured reflections	2301	2891	2826
observed reflections $I > 3\sigma(I)$	1993	1525	2613
θ_{max} (deg)	65	24	70
h_{min}, h_{max}	0, 31	0, 12	0, 10
k_{min}, k_{max}	0, 8	0, 8	−11, 11
l_{min}, l_{max}	−17, 17	−24, 24	−13, 13
no. of intensity control reflections, frequency, and variation	3, every 1 h, nil	3, every 1 h, nil	3, every 1 h, nil
no. of orientation control reflections, frequency, and variation	3, every 200 reflns, nil	3, every 200 reflns, nil	3, every 200 reflns, nil
	Refinement		
refinement on	$\|F\|$	$\|F\|$	$\|F\|$
final R	0.038	0.066	0.039
weighted R	0.058	0.067	0.059
reflections used	1993	1525	2613
no. of parameters in the least-squares refinement	190	230	208
hydrogen atom positions	not refined	not refined	not refined
$(\Delta/\sigma)_{max}$	0.01	0.02	0.04
weighting scheme, w	$1/\sigma(F)^2$	$1/\sigma(F)^2$	$1/\sigma(F)^2$
$\Delta\rho_{max}$ (e Å^{-3})	+0.53	+1.00	+0.35
$\Delta\rho_{min}$ (e α^{-3})	−0.45	−0.64	−1.00
extinction correction	not applied	not applied	not applied
source of atomic scattering factors	*International Tables for X-ray Crystallography* (1974, Vol. IV)		

Cu···Cu′ distance shows only a marginal increase from **1** (Cu···O1′ = 2.801(7) Å, Cu···Cu′ = 3.266(7) Å, ∠Cu–O1···Cu′ = 85.7(7)° and ∠O1′···Cu–O1 = 94.3(7)°. Coordination geometry around copper is highly distorted square-pyramidal with almost coplanar N_2O_2 atoms forming a basal plane and with a long Cu···O1′ apical bond. The displacement of Cu atom from this plane is negligibly small (0.06 Å). It is noteworthy that although the ethylenediamine conformation is identical to **1** with C8 out by 0.47 Å and C9 by 0.09 Å from the CuN1N2 plane, the molecule is essentially planar. "sal1" and "sal2" planes bend symmetrically making angles of 14.5(5)° and 9.9(7)°, respectively, with the N_2O_2 plane. The planar conformation could be because of the weaker Cu···O1′ bond (2.801(7) Å) in **2** which reduces the steric interaction between benzene rings as opposed to **1**. Interestingly, chloroform adduct of Cu(salen) with a dimer bond a little shorter than in **2** (Cu···O1′ = 2.79 Å) has a "stepped" conformation. This brings out the fact that the ethylenediamine conformation and the overall molecular geometry are not necessarily interrelated as thought previously,[25] further demonstrating the flexibility of the "salen" framework. The packing of molecules in **2** creates channels because of the protruding methoxy groups, in which a methanol is included. As discussed in the Experimental Section, the solvent molecule is disordered and the disordered oxygen O101 and O102 make H-bonding contacts with O2 of the ligand not involved in dimer formation (O101···O2 = 2.90 Å and O102···O2 = 2.65 Å). The H-bonding interaction of the solvent molecule in the lattice with the ligand is observed to be one of the factors influencing dimeric association. This is best exemplified by the X-ray structures of Cu(salen) (strong dimer) and its adducts with chloroform (weak dimer)[26] and nitrophenol (monomer).[25]

Chloro-substituted Cu(salen) **3** also has a molecular association across the center of symmetry as in **1** and **2** but Cu···O1′ = 3.307(2) Å; Cu···Cu′ = 3.502(2) Å is too long to be considered as a dimer. Moreover, the angles ∠Cu–O1···Cu′(79.5(1)°) and ∠O1′···Cu–O1 (68.2(1)°) show considerable shearing of molecules. The donor atoms N_2O_2 do not form a perfect plane but deviate by ∼±0.11 Å from their best plane to form a tetrahedrally distorted square planar geometry around Cu. Atoms C8 and C9 are displaced by 0.39 and 0.22 Å, respectively, in opposite directions from the CuN1N2 plane. The "sal" units are twisted with respect to each other (twist angle = 9.4(4)°) and make angles 11.5(2)° and 8.2(3)° with the best plane of the donor atoms. The two Cu–O bonds are similar and compare well with the literature values.[25,26] But, Cu–N distances in **3** are somewhat

(25) Baker, E. N.; Hall, D.; Waters, T. N. *J. Chem. Soc. A* **1970**, 400.

Table II. Positional Parameters and Their Estimated Standard Deviations[a]

atom	x	y	z	B (Å²)	atom	x	y	z	B (Å²)
				Complex 1					
Cu	0.23284(1)	0.20565(5)	0.09795(2)	2.087(8)	C7	0.3304(1)	0.0217(4)	0.1442(2)	2.95(6)
O1	0.28454(7)	0.3765(3)	0.0624(1)	2.32(4)	C8	0.2588(1)	−0.1824(4)	0.1405(2)	3.39(7)
O2	0.18423(7)	0.4082(3)	0.0889(1)	2.71(4)	C9	0.2134(1)	−0.1438(4)	0.1920(2)	3.06(6)
N1	0.28275(9)	0.0020(3)	0.1274(2)	2.56(5)	C10	0.1421(1)	0.0615(4)	0.1644(2)	2.82(6)
N2	0.18799(9)	0.0311(3)	0.1536(2)	2.53(4)	C11	0.1143(1)	0.2327(4)	0.1377(2)	2.76(6)
C1	0.3334(1)	0.3637(4)	0.0904(2)	2.44(5)	C12	0.0627(1)	0.2375(5)	0.1504(3)	4.03(7)
C2	0.3643(1)	0.5215(5)	0.0781(2)	3.19(6)	C13	0.0332(1)	0.3968(6)	0.1269(3)	4.60(8)
C3	0.4160(1)	0.5188(6)	0.1048(3)	4.26(8)	C14	0.0544(1)	0.5541(6)	0.0908(3)	4.05(7)
C4	0.4389(1)	0.3563(7)	0.1465(3)	4.67(8)	C15	0.1051(1)	0.5561(5)	0.0786(2)	3.38(6)
C5	0.4105(1)	0.2003(5)	0.1590(3)	3.90(7)	C16	0.1370(1)	0.3971(4)	0.1015(2)	2.46(5)
C6	0.3575(1)	0.1972(4)	0.1319(2)	2.77(6)					
				Complex 2					
Cu	0.52494(9)	0.7995(1)	0.52613(4)	2.64(1)	C7	0.4165(7)	0.709(1)	0.4062(4)	3.4(1)
O1	0.6230(6)	0.9005(8)	0.4659(3)	3.5(1)	C8	0.2922(7)	0.673(2)	0.4907(5)	4.6(2)
O2	0.6429(4)	0.8573(8)	0.5892(3)	3.2(1)	C9	0.3200(8)	0.591(1)	0.5523(5)	3.7(1)
O3	0.6277(6)	0.796(1)	0.2156(3)	4.3(1)	C10	0.4333(7)	0.696(1)	0.6423(3)	3.1(1)
O4	0.6140(7)	0.879(1)	0.8397(3)	4.2(1)	C11	0.5307(6)	0.780(1)	0.6774(3)	2.8(1)
O101	0.109	0.082	0.443	5.3(3)*	C12	0.5274(6)	0.785(1)	0.7407(3)	3.2(1)
O102	0.141	0.043	0.445	7.3(5)*	C13	0.6125(8)	0.866(1)	0.7779(4)	3.5(1)
N1	0.4086(6)	0.714(1)	0.4627(3)	3.6(1)	C14	0.7095(7)	0.941(1)	0.7506(4)	3.3(1)
N2	0.4208(5)	0.6866(9)	0.5833(3)	3.1(1)	C15	0.7170(7)	0.936(1)	0.6863(4)	3.1(1)
C1	0.6198(7)	0.867(1)	0.4077(3)	2.8(1)	C16	0.6316(7)	0.8550(9)	0.6478(4)	2.9(1)
C2	0.7110(8)	0.925(1)	0.3707(4)	3.6(1)	C17	0.5305(9)	0.721(1)	0.1804(4)	4.1(2)
C3	0.7138(9)	0.904(1)	0.3094(4)	3.9(2)	C18	0.509(1)	0.827(2)	0.8686(4)	4.5(2)
C4	0.6164(7)	0.811(1)	0.2775(4)	3.5(1)	C101	0.082	0.209	0.471	6.9(6)*
C5	0.5241(7)	0.7493(9)	0.3117(3)	2.8(1)	C102	0.082	0.209	0.484	5.0(3)*
C6	0.5227(6)	0.7713(8)	0.3762(4)	2.6(1)					
				Complex 3					
Cu	0.51180(4)	0.13313(3)	0.06709(3)	2.874(7)	C6	0.6513(3)	−0.2285(2)	0.2566(2)	2.92(4)
Cl1	0.94359(9)	−0.62272(7)	0.43377(7)	4.50(2)	C7	0.4775(3)	−0.1795(3)	0.2866(2)	3.16(5)
Cl2	0.2598(1)	0.94092(8)	−0.36906(8)	5.02(2)	C8	0.2260(3)	−0.0074(3)	0.2579(3)	3.59(6)
O1	0.7179(2)	0.0082(2)	0.0514(2)	4.08(4)	C9	0.1981(3)	0.1626(3)	0.2383(2)	3.63(6)
O2	0.5905(2)	0.3073(2)	−0.0984(2)	3.32(4)	C10	0.2583(3)	0.3976(3)	0.0349(2)	3.30(5)
N1	0.4066(2)	−0.0427(2)	0.2222(2)	3.14(4)	C11	0.3520(3)	0.4978(3)	−0.0935(2)	3.15(5)
N2	0.3050(2)	0.2539(2)	0.1077(2)	3.08(4)	C12	0.2785(3)	0.6506(3)	−0.1598(2)	3.58(5)
C1	0.7621(3)	−0.1326(3)	0.1404(2)	3.13(5)	C13	0.3550(3)	0.7514(3)	−0.2867(2)	3.69(5)
C2	0.9308(3)	−0.1971(3)	0.1208(2)	3.65(6)	C14	0.5078(3)	0.7021(3)	−0.3513(2)	3.68(5)
C3	0.9867(3)	−0.3427(3)	0.2088(3)	3.56(5)	C15	0.5823(3)	0.5552(3)	−0.2870(2)	3.52(5)
C4	0.8738(3)	−0.4350(3)	0.3214(2)	3.27(5)	C16	0.5100(3)	0.4451(3)	−0.1537(2)	3.00(5)
C5	0.7107(3)	−0.3789(3)	0.3445(2)	3.17(5)					

[a] Anisotropically refined atoms are given in the form of the isotropic equivalent displacement parameter defined as: $(4/3)[a^2B(1,1) + b^2B(2,2) + c^2B(3,3) + ab(\cos\gamma)B(1,2) + ac(\cos\beta)B(1,3) + bc(\cos\alpha)B(2,3)]$. Starred values were refined isotropically.

shorter than in **1** (Table III), perhaps due to decrease in the coordination number of Cu from 5 to 4. The weaker dimer association in **2** was rationalized in terms of the solvent H-bonding interaction with the ligand, but no dimeric interaction in the absence of any solvent molecule in **3** could only be attributed to the chlorine substitution.

EPR Studies. The EPR spectra for polycrystalline samples of **1–3**, at 298 and 77 K are very similar (Figure 3) and characterized by an axial **g** tensor with $g_\parallel > g_\perp$. The principal g values calculated using the method of Kneubuhl[27] (Table IV) are in agreement with those reported for bidentate Cu(II) Schiff base complexes[28–30] suggesting that the unpaired electron occupies a "formal" d_{xy} orbital. Hyperfine coupling due to the metal ion (A_{Cu})[31] could not be resolved even at 77 K due to exchange narrowing of EPR lines.

The substituents (X) and molecular geometry have significant effect on both $g_\parallel$ and $g_\perp$ values. As seen from Table IV, **1** and **2** have almost the same $g_\perp$ value whereas **3** has a much lower value. Further, the line width for the $g_\perp$ feature is relatively smaller for **3** (~50 G) than for **1** and **2** (~85 G). But the $g_\parallel$ values vary in the order **1** > **2** > **3**. The variations in $g_\parallel$ could be interpreted due to the changes in the coordination number and intermolecular Cu···O1′ distances. The increase in $g_\perp$ value can be correlated with the distortions from the square planarity of N_2O_2.

The increase in the principal **g** components with lowering of temperature to 77 K indicates small changes in the molecular conformation. The absence of characteristic signals due to dimers in **1** and **2** is due to weak magnetic interactions between two copper units intermolecularly bridged by phenolate oxygen.

Color Isomerism and Solvatochromism. Complexes **1–3** show color isomerism in solid state. Complex **1** gave green solid from alcohol while green and deep red solids were obtained from chloroform. The green compound is analyzed in the present study as dimeric Cu(salen) whereas the deep red product was characterized by Waters and Hall[26] as a chloroform adduct of dimeric Cu(salen). Methanolic solutions of **2** and **3** yielded wine red and brown crystals while their ethanolic solutions yielded green crystals. Single crystals of **2** and **3** exhibit dichroism by showing different colors in reflected and transmitted lights. However, these color isomers did not show any marked spectral changes.

Complexes exhibit solvatochromism; the color of the solution changes from violet through blue to green as the σ donation capability of the solvent[32] increases (Table IV). Waters and

(26) Baker, E. N.; Hall, D.; Waters, T. N. *J. Chem. Soc. A* **1970**, 406.
(27) Kneubühl, F. K. *J. Chem. Phys.* **1960**, *33*, 1074.
(28) Maki, A. H.; McGarvey, B. R. *J. Chem. Phys.* **1958**, *29*, 31 and 35. McGarvey, B. R. *J. Phys. Chem.* **1956**, *60*, 71.
(29) Gresmann, H. R.; Swalen, J. D. *J. Chem. Phys.* **1962**, *36*, 3221. Kivelson, D.; Neiman, R. *J. Chem. Phys.* **1961**, *35*, 149.
(30) Hasty, E.; Colburn, T. J.; Hendrickson, D. N. *Inorg. Chem.* **1973**, *12*, 2414. Bertini, I.; Canti, G.; Grassi, R.; Scozzafava, A. *Inorg. Chem.* **1980**, *19*, 2198. Hitchman, M. A.; Olson, C. D.; Belford, R. C. *J. Chem. Phys.* **1968**, *50*, 1195.
(31) Copper has two magnetic nuclei ^{63}Cu and ^{65}Cu with nuclear gyromagnetic ratios (g_N) being 1.484 and 1.588 and abundances being 69.2% and 30.8%, respectively; both the nuclei have a spin of $I = {}^3/_2$.

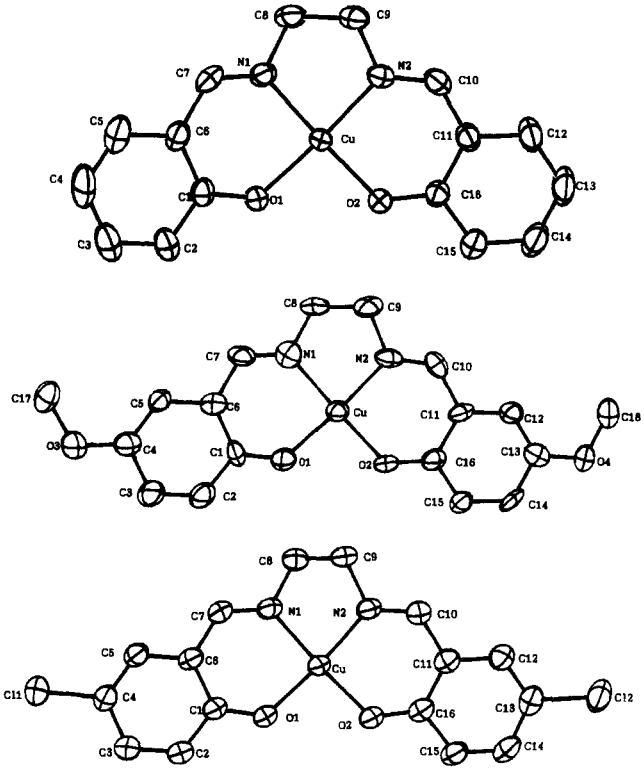

Figure 1. ORTEP views of (a, top) Cu(salen), (b, middle) Cu(5-CH_3O-salen), and (c, bottom) Cu(5-Cl-salen).

Hall[33] have reported color changes for Cu(II) Schiff bases in a few solvents attributing violet and brown colors to tetracoordination and green color to strong pentacoordination of copper.[34] However, this color rule does not hold good for all the copper complexes[26,35] as various other factors (*vide infra*) influence the chromic properties.

The electronic spectra of the complexes are similar in various solvents, but the charge transfer (~380 nm) and d–d (~565 nm) bands shift to higher wavelengths as the basicity of the solvent increases. Cyclic voltammetry of **1–3** indicate the solvent effect on the redox couples of I and II. The anodic and cathodic waves of couple II (Cu(II)/Cu(I)) shift to negative potentials with the increase in the donacity of the solvent. In a highly σ-donor solvent, py, couple I shifts to more positive potentials.

The EPR spectra of **1–3** at 298 K in solution show four equally spaced resonances attributable to the interaction of electron spin with the nuclear spin of Cu(II). But ^{63}Cu and ^{65}Cu hyperfine features could not be resolved. The resonances show m_I dependent line widths,[36] with the high field line being narrower and more intense than the low field line. Representative spectra for **2** are shown in Figure 4. The isotropic g and A_{Cu} calculated by spectral fitting are listed in Table IV.

Figure 5 shows good correlations between g_{iso} and A_{iso}, and g_{iso} and the Gutmann donor number (DN).[32] With increasing donor capacity of the solvent, the g_{iso} value increases with a concomitant decrease in the magnitude of the A_{iso}. These agree with the changes in electronic spectral data and $E_{1/2}$ values for couple II implying the decrease in ligand field splitting with increase in σ basicity of the solvent. The deviation observed for py should be due to its strong coordination to copper.

The superhyperfine splitting with about 15 lines on the high field isotropic copper hyperfine feature (Figure 4) cannot be attributed to the interaction with two equivalent ^{14}N nuclei alone, but the splittings and the line intensities could be very well accounted for the interaction of two equivalent proton spins along with the two ^{14}N nuclei. The superhyperfine coupling parameters were calculated to be $A_N(iso) = 13.9 \times 10^{-4}$ cm^{-1} and $A_H(iso) = 7.5 \times 10^{-4}$ cm^{-1}. The protons here belong to the carbon atoms adjacent to ^{14}N nuclei. Similar observations were reported for some bidentate salicylidinimine Schiff base Cu(II) complexes.[28]

EPR spectra of frozen solutions of **1–3** at 77 K are characterized by axial **g** and **A** tensors (Figure 3). Three of the four parallel hyperfine features are well resolved while the fourth one is overlapped by $g_\perp$ features which are partially resolved. Apart from this an extra line indicated by an asterisk (*) for frozen glasses is an "angular anomaly" due to powder averaging.[29] The superhyperfine features at 298 K were not seen in the frozen solution spectra except for pyridine. The $g_\parallel$, $g_\perp$, and $A_\parallel$ values could be readily calculated from the spectra. However, the accuracy of $A_\perp$ values is lower because of the partially resolved perpendicular features. As the σ basicity or DN of the solvent increases, the $g_\parallel$ values increase whereas $A_\parallel$ values decrease (Table IV).

Ground-State Wave Function and Bonding Parameters. The spin Hamiltonian parameters (Table IV) indicate that the unpaired electron occupies a "formal" d_{xy} orbital. The MO coefficients have been calculated using the ligand field approach adopted by Maki and McGarvey[28] and later by Kivelson and Neiman[29] for a D_{2h} symmetry. α and β are metal d orbital coefficients for the MOs B_{1g} and A_g, representing the in-plane σ and π bonding, respectively; δ is the coefficient for the MO E_g representing the out-of-plane π bonding and α' is the coefficient for ligand orbitals forming the B_{1g} orbital. The MO coefficients listed in Table V were obtained by using the value of –828 cm^{-1} for λ, the spin–orbit coupling constant, and 0.036 cm^{-1} for P, the dipolar interaction term for free Cu(II) ion. The overlap integral S and the constant $T(n)$ were assumed as 0.093 and 0.333, respectively. A clear excitation band for $B_{1g} \leftrightarrow A_g$ was observed for all the complexes in the range 16750–17699 cm^{-1}. However, the d–d band for $B_{1g} \leftrightarrow E_g$ was not observed in all the cases, as it overlapped by a charge transfer band. Therefore, the coefficient δ was calculated only in those cases where this band was observed. The MO coefficients (Table V) suggest that the in-plane σ and π bondings are covalent while the out-of-plane π bonding is ionic in nature. The present study shows marked changes in the in-plane π bonding with substitution and solvent as observed by Kivelson and Neiman for several Cu(II) complexes.[29] The α^2 values decrease in the order **1** > **2** > **3** while the β^2 values increase in the same order. Similar variations in α^2 and β^2 values are observed with increasing σ-basicity of the solvent. Although the in-plane σ and π bonding parameters are equally important, the latter is probably a better indicator of covalent bonding. The extra superhyperfine coupling due to ^{14}N nuclei in solvents ($A_N(iso) = 13.9 \times 10^{-4}$ cm^{-1}) has yielded an indirect estimate of 0.771 and 0.322 for α^2 and α'^2, respectively. These are in agreement within experimental errors with those listed in Table V.

EHMO calculations were carried out on **1–3** by the method described by Hoffmann[37] using the positional parameters from X-ray studies. However, as the basis set was very large to handle, calculations were performed on acacen type model systems; we believe such a simplification should not alter the results significantly. The off-diagonal elements were calculated using a weighted Wolfberg–Helmholz formula[38] with the Hückel constant of 1.75. The input parameters, such as Coulomb integrals and

(32) Gutmann donor number (DN) was chosen as a measure of the Lewis basicity of solvent molecules. Gutmann, V. *The Donor-Acceptor Approach to Molecular Interactions*; Plenum Press: New York, 1978. Gutmann, V. *Coordination Chemistry in Non-aqueous Solutions*; Springer: Vienna, 1968.
(33) Waters, T. N.; Hall, D. J. *J. Chem. Soc.* **1959**, 1200.
(34) Llewellyr, F. J.; Waters, T. N. *J. Chem. Soc.* **1960**, 2639.
(35) Hall, D.; Sheat, S. V.; Waters, T. N. *J. Chem. Soc.* **1968**, 460.
(36) Lewis, W. B.; Morgan, L. O. *Transition Metal Chemistry*; Carlin, R. L., Ed.; Marcel Dekker: New York, 1968, Vol. 4, p 33.
(37) Hoffmann, R. *J. Chem. Phys.* **1963**, *39*, 1397. Hoffmann, R.; Lipscomb, W. N. *J. Chem. Phys.* **1962**, *37*, 177.
(38) McGlynn, S. P.; Vanquickenborne, L. G.; Kinoshita, M.; Carroll, D. G. *Introduction to Applied Quantum Chemistry*; Holt, Reinhart and Winston: New York, 1972.

Table III. Bond Distances in Angstroms and Bond Angles in Degrees[a]

Complex **1**

atom 1	atom 2	distance	atom 1	atom 2	distance	atom 1	atom 2	distance
Cu	O1	1.945(2)	N2	C10	1.273(4)	C10	C11	1.434(4)
Cu	O2	1.911(2)	C1	C2	1.401(4)	C11	C12	1.413(4)
Cu	N1	1.958(2)	C1	C6	1.426(4)	C11	C16	1.431(4)
Cu	N2	1.959(2)	C2	C3	1.382(4)	C12	C13	1.380(5)
O1	C1	1.319(4)	C3	C4	1.393(6)	C13	C14	1.374(6)
O2	C16	1.299(3)	C4	C5	1.354(6)	C14	C15	1.385(5)
N1	C7	1.271(4)	C5	C6	1.419(4)	C15	C16	1.412(4)
N1	C8	1.460(4)	C6	C7	1.444(4)			
N2	C9	1.474(4)	C8	C9	1.533(5)			

atom 1	atom 2	atom 3	angle	atom 1	atom 2	atom 3	angle	atom 1	atom 2	atom 3	angle
O1	Cu	O2	91.43(9)	C9	N2	C10	119.5(3)	N2	C9	C8	108.0(3)
O1	Cu	N1	91.16(9)	O1	C1	C2	118.7(3)	N2	C10	C11	125.1(3)
O1	Cu	N2	170.40(8)	O1	C1	C6	124.1(3)	C10	C11	C12	117.4(3)
O2	Cu	N1	171.3(1)	C2	C1	C6	117.2(2)	C10	C11	C16	122.9(3)
O2	Cu	N2	92.56(9)	C1	C2	C3	122.2(4)	C12	C11	C16	119.8(3)
N1	Cu	N2	83.7(1)	C2	C3	C4	120.1(3)	C11	C12	C13	121.3(3)
Cu	O1	C1	125.5(2)	C3	C4	C5	119.6(4)	C12	C13	C14	119.4(3)
Cu	O2	C16	127.4(2)	C4	C5	C6	122.0(3)	C13	C14	C15	121.0(3)
Cu	N1	C7	126.8(3)	C1	C6	C5	118.9(3)	C14	C15	C16	121.9(3)
Cu	N1	C8	112.0(2)	C1	C6	C7	122.9(2)	O2	C16	C11	124.4(3)
C7	N1	C8	120.8(2)	C5	C6	C7	118.2(3)	O2	C16	C15	118.9(3)
Cu	N2	C9	113.6(2)	N1	C7	C6	124.8(3)	C11	C16	C15	116.7(3)
Cu	N2	C10	126.7(3)	N1	C8	C9	107.2(2)				

Complex **2**

atom 1	atom 2	distance	atom 1	atom 2	distance	atom 1	atom 2	distance
Cu	O1	1.908(6)	N1	C7	1.24(2)	C6	C7	1.46(2)
Cu	O2	1.895(5)	N1	C8	1.49(1)	C8	C9	1.49(1)
Cu	N1	1.948(7)	N2	C9	1.47(2)	C10	C11	1.43(1)
Cu	N2	1.942(7)	N2	C10	1.286(9)	C11	C12	1.38(2)
O1	C1	1.290(9)	C1	C2	1.40(1)	C11	C16	1.45(2)
O2	C16	1.29(2)	C1	C6	1.44(2)	C12	C13	1.36(1)
O3	C4	1.36(2)	C2	C3	1.35(1)	C13	C14	1.38(1)
O3	C17	1.41(1)	C3	C4	1.43(1)	C14	C15	1.41(1)
O4	C13	1.35(2)	C4	C5	1.38(1)	C15	C16	1.38(2)
O4	C18	1.41(1)	C5	C6	1.41(2)			

atom 1	atom 2	atom 3	angle	atom 1	atom 2	atom 3	angle	atom 1	atom 2	atom 3	angle
O1	Cu	O2	90.4(3)	C9	N2	C10	121.7(7)	N2	C9	C8	109.0(8)
O1	Cu	N1	91.6(3)	O1	C1	C2	121.6(7)	N2	C10	C11	126.4(7)
O1	Cu	N2	176.4(3)	O1	C1	C6	123.0(8)	C10	C11	C12	118.8(6)
O2	Cu	N1	173.9(3)	C2	C1	C6	115.4(7)	C10	C11	C16	121.1(7)
O2	Cu	N2	92.9(3)	C1	C2	C3	126.2(8)	C12	C11	C16	120.1(7)
N1	Cu	N2	85.0(3)	C2	C3	C4	118.6(9)	C11	C12	C13	123.4(7)
Cu	O1	C1	127.6(5)	O3	C4	C3	114.1(8)	O4	C13	C12	126.6(8)
Cu	O2	C16	127.7(5)	O3	C4	C5	128.0(8)	O4	C13	C14	115.8(8)
C4	O3	C17	117.4(8)	C3	C4	C5	117.8(7)	C12	C13	C14	117.6(8)
C13	O4	C18	117.5(7)	C4	C5	C6	123.0(7)	C13	C14	C15	120.6(7)
Cu	N1	C7	129.2(6)	C1	C6	C5	118.8(6)	C14	C15	C16	122.8(7)
Cu	N1	C8	109.6(5)	C1	C6	C7	123.5(7)	O2	C16	C11	124.7(7)
C7	N1	C8	120.7(7)	C5	C6	C7	117.4(6)	O2	C16	C15	119.7(7)
Cu	N2	C9	112.9(6)	N1	C7	C6	122.6(7)	C11	C16	C15	115.5(7)
Cu	N2	C10	125.4(5)	N1	C8	C9	108.1(7)				

Complex **3**

atom 1	atom 2	distance	atom 1	atom 2	distance	atom 1	atom 2	distance
Cu	O1	1.904(2)	N1	C8	1.467(3)	C6	C7	1.433(3)
Cu	O2	1.911(1)	N2	C9	1.474(3)	C8	C9	1.511(4)
Cu	N1	1.943(2)	N2	C10	1.281(3)	C10	C11	1.437(3)
Cu	N2	1.945(2)	C1	C2	1.423(3)	C11	C12	1.398(3)
Cl1	C4	1.748(2)	C1	C6	1.424(3)	C11	C16	1.422(3)
Cl2	C13	1.748(2)	C2	C3	1.363(3)	C12	C13	1.374(3)
O1	C1	1.310(2)	C3	C4	1.403(3)	C13	C14	1.398(3)
O2	C16	1.300(2)	C4	C5	1.363(3)	C14	C15	1.358(4)
N1	C7	1.280(3)	C5	C6	1.402(3)	C15	C16	1.435(3)

atom 1	atom 2	atom 3	angle	atom 1	atom 2	atom 3	angle	atom 1	atom 2	atom 3	angle
O1	Cu	O2	91.63(6)	O1	C1	C2	118.9(2)	N2	C9	C8	107.5(3)
O1	Cu	N1	92.63(7)	O1	C1	C6	124.3(2)	N2	C10	C11	125.0(3)
O1	Cu	N2	172.41(9)	C2	C1	C6	116.8(2)	C10	C11	C12	116.7(2)
O2	Cu	N1	171.8(1)	C1	C2	C3	122.5(2)	C10	C11	C16	122.4(2)
O2	Cu	N2	92.98(6)	C2	C3	C4	119.2(3)	C12	C11	C16	120.8(2)
N1	Cu	N2	83.56(8)	Cl1	C4	C3	119.7(2)	C11	C12	C13	120.7(2)
Cu	O1	C1	127.3(1)	Cl1	C4	C5	119.8(1)	Cl2	C13	C12	120.0(2)
Cu	O2	C16	127.0(1)	C3	C4	C5	120.6(2)	Cl2	C13	C14	119.7(2)
Cu	N1	C7	126.8(1)	C4	C5	C6	121.1(2)	C12	C13	C14	120.3(2)
Cu	N1	C8	112.6(1)	C1	C6	C5	119.9(2)	C13	C14	C15	119.8(2)
C7	N1	C8	120.5(2)	C1	C6	C7	122.6(2)	C14	C15	C16	122.7(3)
Cu	N2	C9	112.8(1)	C5	C6	C7	117.7(2)	O2	C16	C11	125.4(2)
Cu	N2	C10	127.0(1)	N1	C7	C6	125.2(2)	O2	C16	C15	118.8(2)
C9	N2	C10	120.2(2)	N1	C8	C9	106.4(3)	C11	C16	C15	115.8(2)

[a] Numbers in parentheses are estimated standard deviations in the least significant digits.

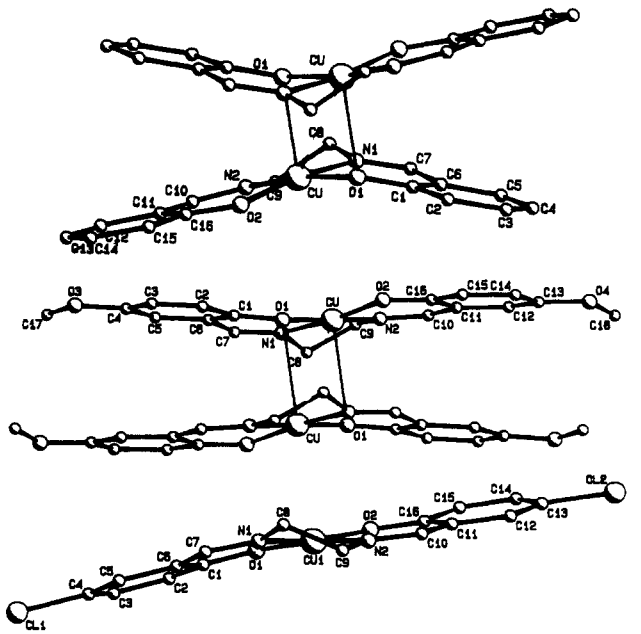

Figure 2. Diagrams illustrating the effect of substitutions on molecular association and chelate conformation: (a, top) dimers of Cu(salen) in "stepped" conformation (Cu···O1′ = 2.414(2) Å and Cu···Cu′ 3.1962(2) Å); (b, middle) weak dimers of Cu(5-CH_3O-salen) with a overall planar geometry for salen (Cu···O1′ = 2.801(7) and Cu···Cu′ = 3.266(7) Å); (c, bottom) monomers of Cu(5-Cl-salen).

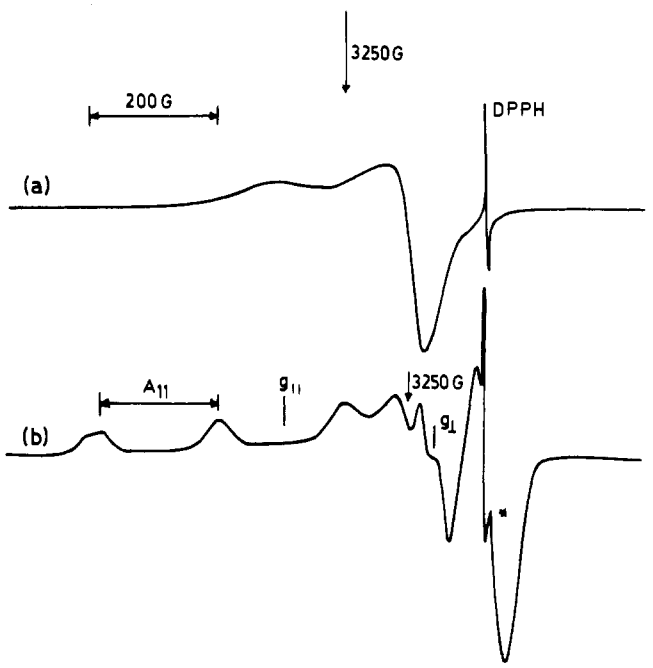

Figure 3. X-band EPR spectra of (a) polycrystalline Cu(5-Cl-salen) at 298 K and (b) Cu(salen) in DMF at 77 K. Asterisk (*) indicates "angular anomaly" due to power averaging.

orbital exponents for Cu, O, N, C, and H, were taken from ref 39. The HOMOs for complexes **1**–**3** are as follows.

$$\psi(1) = -0.898d_{xy} - 0.177d_{z^2} - 0.150d_{x^2-y^2} - 0.240d_{yz}$$

$$\psi(2) = -0.949d_{xy} - 0.120d_{xz}$$

$$\psi(3) = -0.785d_{xy} - 0.375d_{z^2} + 0.130d_{xz} + 0.140d_{yz}$$

In the calculations using the EPR spin Hamiltonian parameters, we have assumed that the ground state is a linear combination of proper ligand orbitals and copper d_{xy} orbital. But the EHMO calculations reveal that the ground-state d_{xy} is admixed with copper d_{z^2} orbital. However, the MO coefficients obtained by both the methods are in excellent agreement. It is interesting to note that as the electron donating power of the substituent decreases changing the geometry of CuN_2O_2 from perfect to tetrahedrally distorted square planar, the HOMO having a predominant d_{xy} character gets increasingly admixed with the d_{z^2} orbital and the electron density at the metal decreases in the order **2** > **1** > **3**.

Mechanisms for Color Isomerism or Solvatochromism. Color isomerism in copper complexes has been the subject of several structural investigations.[25,26,33] Waters and Hall[33] have correlated green color to pentacoordination and brown or violet color to tetracoordination for copper. Complex **1** forms green plates obeying this color rule. However, complex **2** with the same coordination geometry around copper exhibits wine red color. There are a few more exceptions to the color rule like **2**[26,35] suggesting that other parameters like H-bonding interactions between the solvent (guest) and the copper complex (host) also play a vital role. The crystal structures and solution studies further reveal that conformational flexibility of the ligand should also be responsible for changes in the ligand field strength thereby influencing the color, even though there may not be any change in the metal coordination number. Thus color isomerism/solvatochromism exhibited by complexes **1**–**3** can now be understood in terms of not only the fifth coordination of the solvent molecule but involving more subtle molecular features like changes in the ethylenediamine conformation from the equally displaced one (in **3**) to the envelope conformation (in **1** and **2**) as well as weak interactions of the ligand with the solvent molecules (**2**).

Reactivity. The variations of isotropic g and A_{Cu} in several donor solvents (Table IV) reveal that complex **3** is more reactive toward forming pentacoordinated complexes than **1** and **2**. In fact, strong σ donor py forms axial ligand complexes, but the complex with **3** seems to be more stable than with **1** and **2**. EPR spectrum for the py complex of **3** in polycrystalline form recorded immediately after taking out from the mother liquor is characterized by $g_\parallel = 2.223$ and $g_\perp = 2.087$ at 298 K. The higher $g_\parallel$ value than for the parent complex **3** (Table IV) is consistent with the square pyramidal geometry implying axial py coordination. Complexes **1**–**3** clearly demonstrate the conformational flexibility affecting the metal environment achieved by the varying nature of substituents. The higher reactivity of **3** with electron-withdrawing Cl group can be explained in terms of molecular and electronic features as follows: (i) tetrahedrally distorted square planar geometry for copper, (ii) distorted half-chair form for the ethylenediamine ring, and (iii) admixture of electronic ground state d_{xy} with more d_{z^2} orbital and a lower electron density on the metal ion.

It may be mentioned that Cl substitution in salen was reported to form stable py complexes with Ni(III).[40] Also, the Mn(5-Cl-salen) interacted with molecular oxygen forms stable bis(μ-oxo)manganese(IV) complex.[41] In order to probe further into the molecular geometry of the py-bound Cu complexes, attempts to grow X-ray quality crystals are underway. Although, more complex and dynamic situations are encountered in metalloproteins, it is tempting to mention the resemblance of copper environment in **3**, to a certain degree, with that of blue copper proteins[42] and superoxide dismutase.[43]

Concluding Remarks. Flexibility of the salen ligand and fine tuning of the electronic structure by introducing varying electron-donating and electron-withdrawing substituents in Schiff base

(39) Summerville, R. H.; Hoffmann, R. *J. Am. Chem. Soc.* **1976**, *98*, 7240. Albright, T. A.; Hoffmann, P.; Hoffmann, R. *J. Am. Chem. Soc.* **1977**, *99*, 7546.

(40) Castro, B. D.; Freire, C. *Inorg. Chem.* **1990**, *29*, 5113.

(41) Dailey, G. C.; Horwitz, C. P.; Lisek, C. A. *Inorg. Chem.* **1992**, *31*, 5325.

(42) Gray, H. B.; Solomon, E. I. In *Copper Proteins*; Spiro, T. G., Ed.; Wiley-Interscience: New York, 1981. Fee, J. A. *Struct. Bonding (Berlin)* **1975**, *23*, 1. Malkin, R.; Malmstrom, B. G. *Adv. Enzymol.* **1970**, *33*, 177.

(43) McCord, J. M.; Fridovich, I. *J. Biol. Chem.* **1969**, *244*, 6049. Trainer, J. A.; Getzoff, E. D.; Richardson, J. S.; Richardson, D. C. *Nature* **1983**, *306*, 284.

Table IV. EPR Spin Hamiltonian Parameters for Cu(5-X-salen) Complexes

complex	solvent	DN[b]	color	g^c_{iso}	$g_\parallel{}^c$	$g_\perp{}^c$	$A_{Cu}(iso)^d \times 10^{-4}$ cm^{-1}	$A_\parallel{}^d \times 10^{-4}$ cm^{-1}	$A_\perp{}^d \times 10^{-4}$ cm^{-1}
Cu(salen), **1**	solid[a]		green		2.198	2.090			
					(2.191)	(2.084)			
	$CHCl_3$		deep violet	2.0964	2.180	2.054	−88.3	−211.6	−33.5
	CH_2Cl_2	0	bluish violet	2.0986	2.192	2.052	−88.8	−204.7	−33.5
	CH_3CN	14.1	peacock blue	2.0993	2.193	2.052	−87.5	−207.8	−33.5
	DMF	26.6	blue	2.0999	2.212	2.054	−86.0	−203.7	−30.7
	CH_3OH	25.7	green	2.1002	2.214	2.057	−85.0	−201.5	−30.7
	THF	20.0	brownish green	2.1002	2.216	2.056	−84.3	−198.6	−26.9
	pyridine	33.1	green	2.1094	2.227	2.053	−78.5	−191.3	−24.0
Cu(5-CH_3O-salen), **2**	solid[a]		wine red		2.189	2.078			
					(2.188)	(2.082)			
	$CHCl_3$		brownish green	2.0958	2.204	2.047	−88.0	−203.0	−30.6
	CH_2Cl_2	0	green	2.0967	2.209	2.047	−87.7	−203.5	−28.0
	CH_3CN	14.1	green	2.0980	2.211	2.050	−87.7	−203.3	−27.5
	DMF	26.6	green	2.0999	2.213	2.050	−87.2	−201.1	−25.5
	CH_3OH	25.7	brownish green	2.1008	2.216	2.055	−85.7	−198.6	−23.0
	THF	20.0	green	2.1012	2.216	2.057	−85.3	−198.6	−20.5
	pyridine	33.1	green	2.1069	2.226	2.057	−78.3	−193.3	−18.0
Cu(5-Cl-salen), **3**	solid[a]		brown		2.189	2.064			
			red		(2.187)	(2.060)			
	$CHCl_3$		reddish brown	2.0964	2.208	2.057	−88.7	−202.7	−25.6
	CH_2Cl_2	0	green	2.0974	2.212	2.054	−87.8	−201.0	−23.0
	CH_3CN	14.1	blue	2.0990	2.221	2.057	−86.2	−196.2	−18.0
	DMF	26.6	blue	2.1028	2.214	2.055	−85.5	−198.4	−23.0
	CH_3OH	25.7	green	2.1030	2.214	2.055	−84.4	−198.4	−17.9
	THF	20.0		2.1037	2.215	2.054	−84.4	−198.5	−23.0
	pyridine	33.1	green	2.1130	2.231	2.057	−77.8	−188.5	−17.9

[a] Polycrystalline sample: g values in parentheses are those at 77 K. [b] Gutmann donor number. [c] Errors in g_{iso}, $g_\parallel$, and $g_\perp$ are ±0.0005, ±0.001 and ±0.001, respectively. [d] Errors in $A_{Cu}(iso)$, $A_\parallel$, and $A_\perp$ are ±0.5, ±1.0 and ±1.0, respectively.

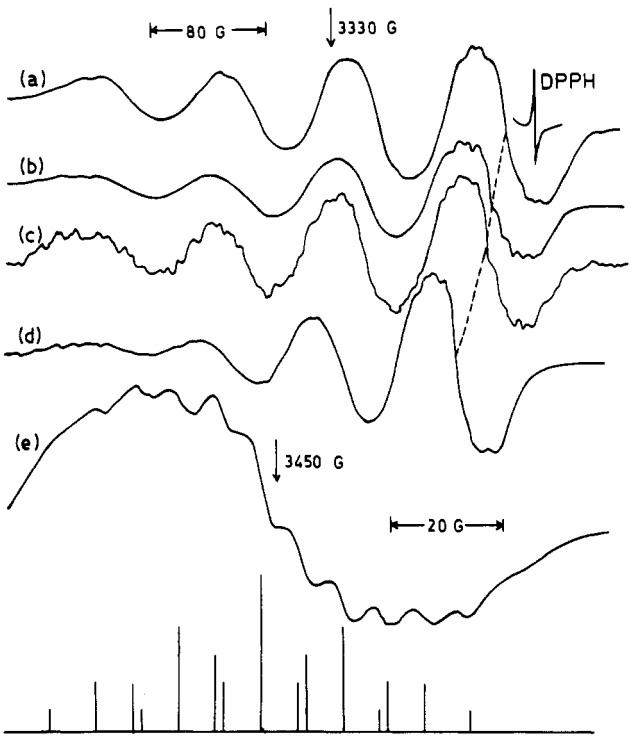

Figure 4. Effect of solvents on the X-band EPR spectra of Cu(5-CH_3O-salen) at 298 K: (a) CH_3CN, (b) DMF, (c) CH_3OH, (d) py, and (e) superhyperfine structure due to two ^{14}N and ^1H nuclei each on the high field side of the copper hyperfine features in (b) and its simulated stick plot.

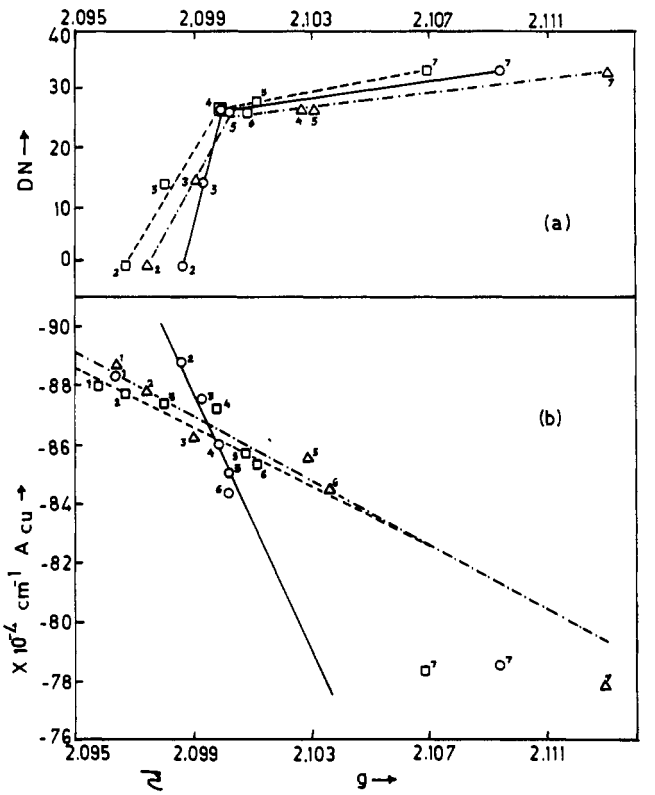

Figure 5. Variations of (a) Gutmann donor number (DN) of the solvents and (b) isotropic copper hyperfine coupling constant (A_{Cu}) with g_{iso}: CH_3CN (1), CH_2Cl_2 (2), $CHCl_3$ (3), DMF (4), CH_3OH (5), THF (6), and py (7); Cu(salen) (——), Cu(5-CH_3O-salen) (– – –), and Cu(5-Cl-salen) (– · –).

and axial ligands are the crucial factors governing the reactivity of the metal center. The present study shows the effect of substituents H, CH_3O, and Cl on molecular association, chelate conformation, and electronic structure. In solid state, complex **1** forms strong dimers with a "stepped" conformation for salen, whereas **2** having an electron-donating CH_3O substituent forms weak dimers with a solvent molecule in the lattice. The overall planarity of **2** with asymmetric ethylenediamine backbone is the first example so far known for the dimeric copper complex. Perhaps, complex **2** demonstrates a delicate balance between a dimeric and a monomeric association. The molecular association described in the crystalline state need not necessarily relate to the thermodynamic stability of complexes in solution. Electron-withdrawing chloro-substituted **3** is essentially a monomer in solid state and distorts the square planar geometry of CuN_2O_2 admixing the ground state d_{xy} orbital with d_{z^2} and thereby enhances the

Table V. Electronic d–d Transitions (cm^{-1}) and Molecular Orbital Coefficients Calculated in D_{2h} Symmetry

complex	solvent	α^2	α'^2	β^2	δ^2	$\Delta E_{x^2-y^2}$	$\Delta E_{xz,yz}$
Cu(salen)	CH_2Cl_2	0.823	0.263	0.698		17 731	
	DMF	0.841	0.243	0.731		17 361	
	CH_3OH	0.838	0.247	0.751		17 699	
	py	0.821	0.266	0.773		16 750	
Cu(5-CH_3O-salen)	CH_2Cl_2	0.835	0.250	0.740		17 699	
	DMF	0.833	0.252	0.747		17 513	
	CH_3OH	0.831	0.254	0.765		17 699	
	py	0.828	0.258	0.764		16 779	
Cu(5-Cl-salen)	CH_2Cl_2	0.834	0.252	0.752	0.972	17 731	24 390
	DMF	0.834	0.257	0.762	0.984	17 361	23 810
	CH_3OH	0.829	0.257	0.769	0.975	17 731	23 529
	py	0.819	0.268	0.789		16 779	

stability of electron-rich axial ligand complexes. It is also seen that color isomerism is related not only to the coordination number of the metal ion but also to the ligand conformational changes vis-a-vis the H-bonding interactions with the solvent molecules. Work on similar lines to examine the effect of substitution on spin-state transition and reactivity toward molecular oxygen by manganese, iron, and cobalt complexes will be reported in the future.

Acknowledgment. The authors acknowledge Dr. G. Ramachandraiah for electrochemical experiments and Professor P. Natarajan for his encouragement and interest in this work.

Supplementary Material Available: Listings of hydrogen atom positions, thermal parameters, bond distances and angles, mean planes, torsion angles analytical and spectroscopic data for ligands and complexes, electrochemical data, cyclic voltammogram for **3**, and packing of molecules (25 pages). Ordering information is given on any current masthead page.